UC Irvine
UC Irvine Previously Published Works

Title
Alfvén eigenmode stability and fast ion loss in DIII-D and ITER reversed magnetic shear plasmas

Permalink
https://escholarship.org/uc/item/13s8k1cs

Journal
Nuclear Fusion, 52(9)

ISSN
0029-5515

Authors
Van Zeeland, MA
Gorelenkov, NN
Heidbrink, WW
et al.

Publication Date
2012-09-01

DOI
10.1088/0029-5515/52/9/094023

Copyright Information
This work is made available under the terms of a Creative Commons Attribution License, availalbe at https://creativecommons.org/licenses/by/4.0/

Peer reviewed

eScholarship.org Powered by the California Digital Library
University of California

IOP Publishing and International Atomic Energy Agency Nuclear Fusion
Nucl. Fusion **52** (2012) 094023 (9pp) doi:10.1088/0029-5515/52/9/094023

Alfvén eigenmode stability and fast ion loss in DIII-D and ITER reversed magnetic shear plasmas

M.A. Van Zeeland[1], N.N. Gorelenkov[2], W.W. Heidbrink[3], G.J. Kramer[2], D.A. Spong[4], M.E. Austin[5], R.K. Fisher[1], M. García Muñoz[6], M. Gorelenkova[2], N. Luhmann[7], M. Murakami[4], R. Nazikian[2], D.C. Pace[1], J.M. Park[4], B.J. Tobias[2] and R.B. White[2]

[1] General Atomics, PO Box 85608 San Diego, CA 92186-5608, USA
[2] Princeton Plasma Physics Laboratory, PO Box 451, Princeton, NJ 08543, USA
[3] University of California-Irvine, University Dr., Irvine, CA, USA
[4] Oak Ridge National Laboratory, Oak Ridge, TN, USA
[5] University of Texas-Austin, 2100 San Jacinto Blvd, Austin, TX 78712-1047, USA
[6] Max-Planck-Institut fur Plasmaphysik, EURATOM Association, Boltzmannstr. 2, D-85748 Garching, Germany
[7] University of California-Davis, 347 Memorial Un, Davis, California 95616, USA

Received 7 February 2012, accepted for publication 1 May 2012
Published 3 September 2012
Online at stacks.iop.org/NF/52/094023

Abstract
Neutral beam injection into reversed-magnetic shear DIII-D plasmas produces a variety of Alfvénic activity including toroidicity-induced Alfvén eigenmodes (TAEs) and reversed shear Alfvén eigenmodes (RSAEs). With measured equilibrium profiles as inputs, the ideal MHD code NOVA is used to calculate eigenmodes of these plasmas. The postprocessor code NOVA-K is then used to perturbatively calculate the actual stability of the modes, including finite orbit width and finite Larmor radius effects, and reasonable agreement with the spectrum of observed modes is found. Using experimentally measured mode amplitudes, fast ion orbit following simulations have been carried out in the presence of the NOVA calculated eigenmodes and are found to reproduce the dominant energy, pitch and temporal evolution of the losses measured using a large bandwidth scintillator diagnostic. The same analysis techniques applied to a DT 8 MA ITER steady-state plasma scenario with reversed-magnetic shear and both beam ion and alpha populations show Alfvén eigenmode instability. Both RSAEs and TAEs are found to be unstable with maximum growth rates occurring for toroidal mode number $n = 6$ and the majority of the drive coming from fast ions injected by the 1 MeV negative ion beams. AE instability due to beam ion drive is confirmed by the non-perturbative code TAEFL. Initial fast ion orbit following simulations using the unstable modes with a range of amplitudes ($\delta B/B = 10^{-5}$–10^{-3}) have been carried out and show negligible fast ion loss. The lack of fast ion loss is a result of loss boundaries being limited to large radii and significantly removed from the actual modes themselves.

(Some figures may appear in colour only in the online journal)

1. Introduction

Alfvén eigenmodes are routinely observed in present tokamaks [1, 2] and are predicted to be unstable in ITER baseline [3] and reversed-magnetic shear scenarios [4]. These modes are routinely observed to cause enhanced transport and even loss of fast ions [5–10], resulting in reductions in fusion performance as well as possible damage to first-wall components [11]. Particularly susceptible to these modes are reversed-magnetic shear plasmas with high minimum safety factor ($q_{\min}$) [12].

A fully self-consistent model of Alfvén eigenmode (AE) stability and non-linear impact on the fast ion profile including redistribution and fast ion loss is an extremely computationally intensive problem. In fact, to capture all the essential processes, the calculations must include fuelling and be carried out for slowing-down timescales—something that is currently intractable. In the interest of creating a reduced model, the approach in this work is to take several components that have been validated elsewhere, or in part here using DIII-D measurements, and apply them in an integrated manner to the problem of fast ion loss by Alfvén eigenmodes in ITER reversed-magnetic shear plasmas. First, we use a measured

 © 2012 IAEA, Vienna Printed in the UK & the USA

or prescribed set of equilibrium profiles (electron density, electron temperature, impurity density, ion temperature, rotation), then calculate the ideal MHD eigenmodes of the plasma as well as the fast ion population whether from injected neutral beam ions or alphas from fusion reactions. The fast ion distribution function is obtained from TRANSP [13] and the ideal MHD eigenmodes from NOVA [14]. Second, the linear stability of the various eigenmodes are calculated perturbatively using NOVA-K [15] and the fast ion population followed in the presence of the unstable modes for a range of amplitudes using both the guiding-centre code ORBIT [16] as well as the full-orbit code SPIRAL [17].

This paper is organized as follows. In section 2.1, a DIII-D discharge showing a range of instabilities and fast ion loss during the current ramp phase is presented and calculations of AE stability are compared favourably to measurements. In section 2.2, modelling of the observed fast ion loss is discussed and it is shown that time periods of loss in this DIII-D discharge occur when eigenmodes extend to loss boundaries present in the plasma. As the current increases, fast ion confinement improves and the more localized modes observed at later times cause little to no measurable loss. In section 3.1, a projected ITER DT steady-state plasma is discussed and both NOVA-K and TAEFL [18, 19] calculations of Alfvén eigenmode stability are presented which show unstable reverse shear Alfvén eigenmodes (RSAEs) and toroidicity-induced Alfvén eigenmodes (TAEs) with toroidal mode numbers in the range $n = 4$–6. Interestingly, both codes predict instability due predominantly to drive from injected 1 MeV beam ions. In section 3.2, simulations of fast ion loss due to the unstable modes in the ITER steady-state plasma are discussed where very little to no loss is found for any reasonable range of amplitudes—a fact which can be explained by connection to the DIII-D results presented in section 2.2. The smaller banana widths in ITER result in loss boundaries only at large radii and removed from the modes. These loss simulations do not include scattering or additional sources of error fields (such as that from test blanket modules (TBMs), toroidal field ripple, or edge localized mode (ELM) mitigation coils) which might significantly modify this result and increase the potential of these AEs to cause loss.

2. Measurements and modelling of Alfvén eigenmodes and fast ion loss in DIII-D

The primary DIII-D discharge discussed here is 142111 [10, 20], which contains a variety of coherent mode activity including TAEs, RSAEs and EGAMs [21], all driven by the injected deuterium beam ions ($E = 80$ keV). This discharge has up to 50% neutron deficit relative to classical TRANSP predictions as well as coherent losses of fast ions at AE frequencies [10, 20]. Fast ion losses are measured using a recently installed large bandwidth pitch angle and energy resolving fast ion loss detector (FILD) [20, 22, 23]. A spectrogram from the central portion of the FILD scintillator during the current ramp phase of this discharge is shown in figure 1(*b*) along with an average spectrum of all ECE data (figure 1(*a*)). This figure shows the large variety of mode activity present in the discharge as well as which modes are responsible for causing coherent/convective losses of fast ions

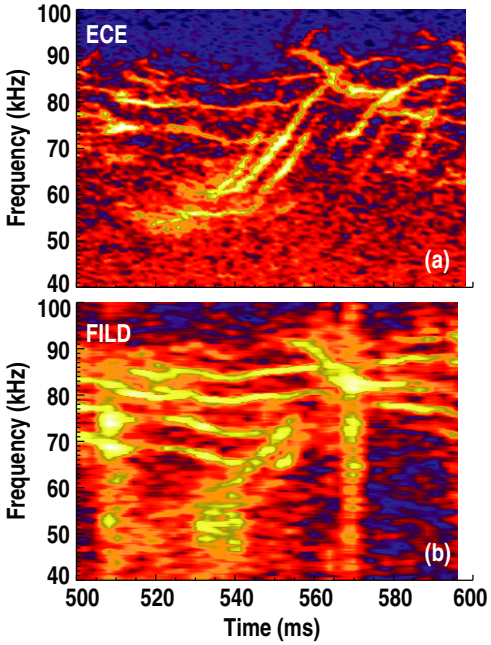

Figure 1. DIII-D Discharge 142111. (*a*) Average spectrogram of several ECE channels on the outboard midplane. (*b*) Fast ion loss detector spectrogram.

(and the relative contribution of the different modes to the loss). TAEs are the series of relatively constant frequency modes above 60 kHz and responsible for the majority of the losses. RSAEs are the modes which sweep up into and across the TAEs.

2.1. Eigenmode stability—DIII-D

Previous analysis has shown excellent agreement between ideal MHD eigenmode structures calculated with NOVA and those measured by the DIII-D radial ECE array [24, 25]. Recently, it was also shown that details of the eigenmode shearing present in experiment can be reproduced by self-consistent inclusion of the effects of the fast ion population on the eigenmode structure, i.e. non-perturbative modelling of the eigenmodes [26, 27]. Despite these detailed structure comparisons, no comparison of eigenmode stability to the actual full measured spectrum of eigenmodes has been carried out. Previous studies on DIII-D have, however, investigated trends elucidating the role thermal ions play in driving Alfvén eigenmodes in high temperature quiescent double barrier plasmas [28] as well as the role that higher order resonances between beam ions and Alfvén eigenmodes play in high $q_{\min}$ plasmas such as the one presented here [12].

Equilibrium profiles of density, temperature, impurity density and rotation are fit and used as inputs to calculate the linear eigenmodes of the plasma with NOVA and the expected beam ion deposition using TRANSP. These profiles as well as the EFIT [29] magnetic equilibrium are shown in figure 2. The pitch angle distribution function shown in figure 2(*d*) is from TRANSP, while the actual beam pressure profile (figure 2(*c*)) is obtained from essentially subtracting the thermal pressure profile from the MSE constrained equilibrium pressure profile (while maintaining charge neutrality). This

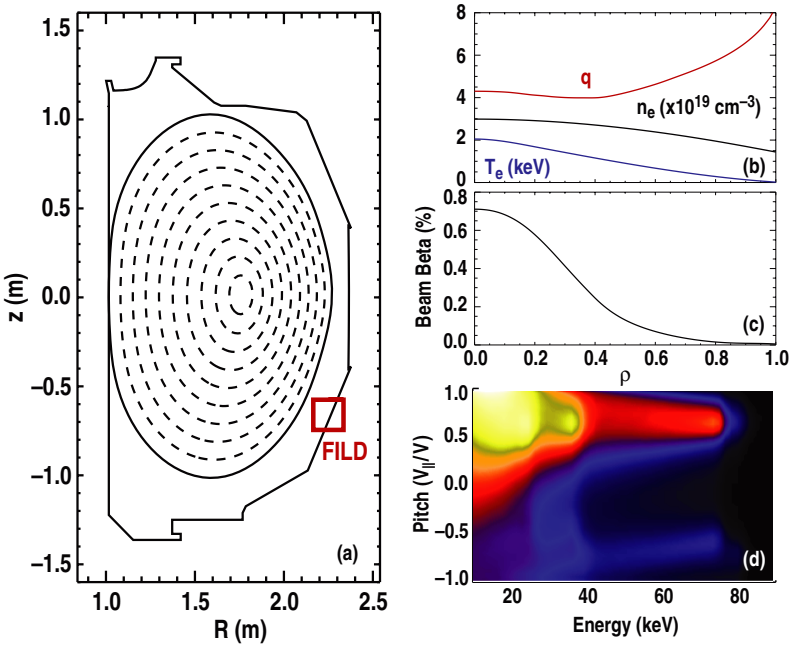

Figure 2. DIII-D Discharge 142111, $t \approx 525$ ms (*a*) EFIT calculated magnetic equilibrium showing FILD location. (*b*) Profiles of safety factor (q), electron density (n_e) and electron temperature (T_e). (*c*) Beam ion pressure profile (*d*) TRANSP calculated beam ion distribution function averaged over the cross-section.

step is necessary since the classical profile from TRANSP does not account for increased transport due to the Alfvén eigenmodes themselves—the result is approximately half the fast ion pressure on-axis expected from classical slowing down [10]. The stability of each eigenmode found with NOVA is then calculated using the code NOVA-K. NOVA-K calculates the drive for each mode based on a solution of the low frequency gyrokinetic equation, where the mode frequency is computed perturbatively using numerical averaging over the fast particle drift orbits. The mode damping in NOVA-K includes the effects of electron collisional, ion/electron Landau, radiative and continuum damping [30].

Classification of the NOVA calculated modes and correspondence with the actual measured modes is carried out using several pieces of information. First, several NOVA runs for a range of $q_{\min}$ values are carried out to identify frequency sweeping indicative of RSAEs. This coupled with localization near $q_{\min}$ and poloidal harmonic content of one or two dominant harmonics is sufficient to classify the modes. Whether a mode corresponds to one observed experimentally is based on frequency (and behaviour with $q_{\min}$), toroidal mode number from a toroidal Mirnov probe array, radial structure from ECE [31], ECEI [32] and poloidal harmonic content from ECEI.

As a representative example, the NOVA calculated $n = 3$ continuum showing the frequency and width of all modes as well as the spatial structure of the calculated unstable and experimentally observed modes are shown in figure 3. Of the four modes predicted to be linearly unstable, two are RSAEs and two are TAEs. Experimentally, there is excellent correspondence with both RSAEs and one of the TAEs. Further comparisons of these modes were made with ECE imaging measurements and are shown in figure 2 of [27].

The results of this process for $n = 2$–6 are given in table 1, where the real frequency, mode type, total drive (with finite Larmor radius corrections), total damping, net growth rate, and whether the mode was observed experimentally are shown for each of the modes calculated to be unstable. Also given in table 1 are the number of unique modes tested for each toroidal mode number, a number which increases with n as expected. All of the modes observed experimentally are identified explicitly in figure 4. Of the 21 modes predicted to be linearly unstable, 10 are observed experimentally. With the exception of $n = 1$, the most unstable mode is observed for each toroidal mode number. For each n, an RSAE is predicted to be the most unstable mode, typically followed by the first radial harmonic such as that shown in blue in figure 3. NOVA-K consistently predicts the fundamental RSAE to be unstable as well as at least one radial harmonic and in some cases the second radial harmonic. Experimentally, at most one radial harmonic is typically observed.

2.2. *Fast ion loss—DIII-D*

A detailed analysis of the fast ion loss induced by Alfvén eigenmodes in this discharge (figure 1(*b*)) was presented in [10]. The key result is reviewed briefly here since it is relevant to the ITER predictions presented in the following sections. The primary theoretical tool used to model fast ion loss in 142111 is the Hamiltonian guiding-centre code ORBIT [16]. ORBIT calculates particle trajectories in a tokamak in the presence of input wavefields superimposed on an equilibrium field. The input eigenmodes are taken from the set of NOVA calculated eigenmodes in table 1 with mode amplitudes fixed to their experimentally observed values. When allowed to operate on the TRANSP calculated distribution function, ORBIT simulations are found to reproduce the dominant energy, pitch and temporal evolution of the FILD measured losses [10]. While loss of both co- and counter-current fast ions

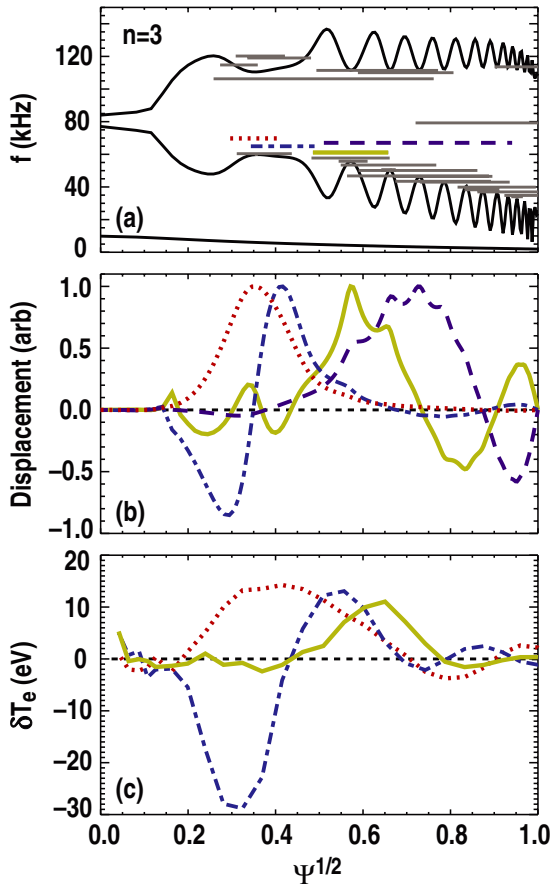

Figure 3. (*a*) NOVA calculated $n = 3$ Alfvénic continuum. Horizontal lines indicate $1/e$ radial extent of eigenmodes and real-frequency. Dashed modes are those calculated by NOVA-K to be unstable. (*b*) Radial structure of displacement envelope on outboard midplane for unstable modes from panel (*a*). (*c*) Radial structure of measured electron temperature perturbation corresponding to experimentally observed $n = 3$ modes. Greyscale shade, (colour online) and linestyle correlates measured modes with calculated modes.

occurs, simulations show that the dominant loss mechanism observed is the mode induced transition of counter-passing fast ions to lost trapped orbits.

Loss simulations for discharge 142111 were carried out for two separate times during the discharge current ramp that exhibit markedly different levels of fast ion loss despite having similar levels of mode activity. The decrease in coherent fast ion loss as the current penetrates as well as the times analysed (vertical shaded bands) are shown in figure 5(*a*). Losses due to TAEs and RSAEs are those occurring in the approximate frequency range 40–100 kHz. ORBIT analysis reproduces this decrease in AE induced fast ion losses at the two times (At $t \approx 525$ ms, $q_{\min} \approx 4$ and $I_p \approx 0.73$ MA, at $t \approx 725$ ms, $q_{\min} \approx 3.33$ and $I_p \approx 0.89$ MA) as well as identified the primary cause for this decay. The loss mechanism itself relies on modes extending to regions near loss boundaries present in the plasma. As the discharge evolves and the current penetrates, fast ion confinement is improved and these loss boundaries move out/away from any mode activity. This improved fast ion confinement combined with the fact that the modes are also becoming more localized (more

Table 1. Modes calculated to be unstable by NOVA-K for discharge 142111 near $t \approx 540$ ms. Table also indicates whether modes were observed experimentally or not. Observed modes are indicated in the spectrogram in figure 4. Drive and damping rates are normalized to mode frequencies.

Freq. (kHz)	Type	Drive	Damp	Drive+damp	Observed
$n = 1$, *Modes tested* $= 19$					
56.26	RSAE	0.162	−0.007	0.154	NO
59.7	TAE	0.021	−0.003	0.017	YES
$n = 2$, *Modes tested* $= 27$					
57.23	RSAE	0.133	−0.027	0.106	YES
62.43	RSAE	0.105	−0.011	0.094	YES
59.98	TAE	0.053	−0.011	0.042	NO
54.63	TAE	0.042	−0.037	0.005	NO
70.83	TAE	0.005	−0.003	0.001	NO
$n = 3$, *Modes tested* $= 28$					
64.92	RSAE	0.101	−0.011	0.089	YES
69.75	RSAE	0.064	−0.003	0.061	YES
61.11	TAE	0.049	−0.029	0.019	YES
67.04	TAE	0.017	−0.011	0.005	NO
$n = 4$, *Modes tested* $= 31$					
76	RSAE	0.052	−0.002	0.05	YES
71.7	RSAE	0.056	−0.008	0.048	NO
68.49	RSAE	0.061	−0.02	0.041	NO
71.76	TAE	0.022	−0.011	0.01	YES
$n = 5$, *Modes tested* $= 38$					
79.71	RSAE	0.056	−0.003	0.053	YES
75.48	RSAE	0.053	−0.007	0.046	NO
72.54	RSAE	0.051	−0.01	0.041	NO
$n = 6$, *Modes tested* $= 46$					
82.8	RSAE	0.033	−0.009	0.024	YES
76.97	RSAE	0.03	−0.018	0.011	NO
74.4	RSAE	0.031	−0.029	0.002	NO

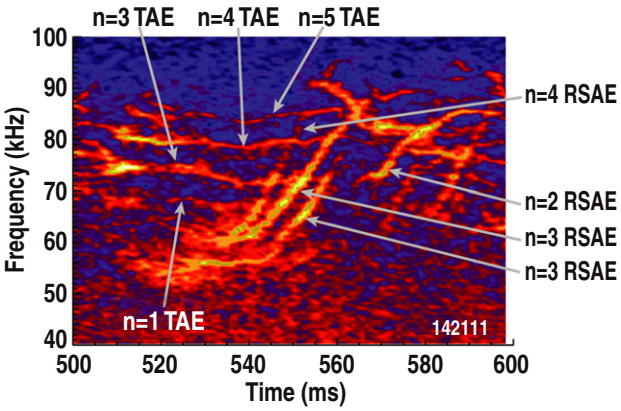

Figure 4. ECE spectrogram from figure 1(*a*) with modes identified for comparison to table 1.

RSAEs and fewer TAEs) results in the fast ion loss becoming significantly reduced. The combination of the effects are shown in figures 5(*b*)–(*e*). Figures 5(*b*) and (*c*) show the various guiding-centre-based orbit topologies for full energy (80 kV) beam ions launched on the outboard midplane with a range of relevant pitch values ($V_\parallel / V$). Particles that fall in the yellow and white regions are on loss trajectories. The innermost extent of the loss boundaries for each case are marked by a vertical dashed line. The actual structure of the various poloidal harmonics used in the simulations are shown in figures 5(*d*) and (*e*). By comparison with the innermost extent of the loss boundaries, it is clear that the modes overlap

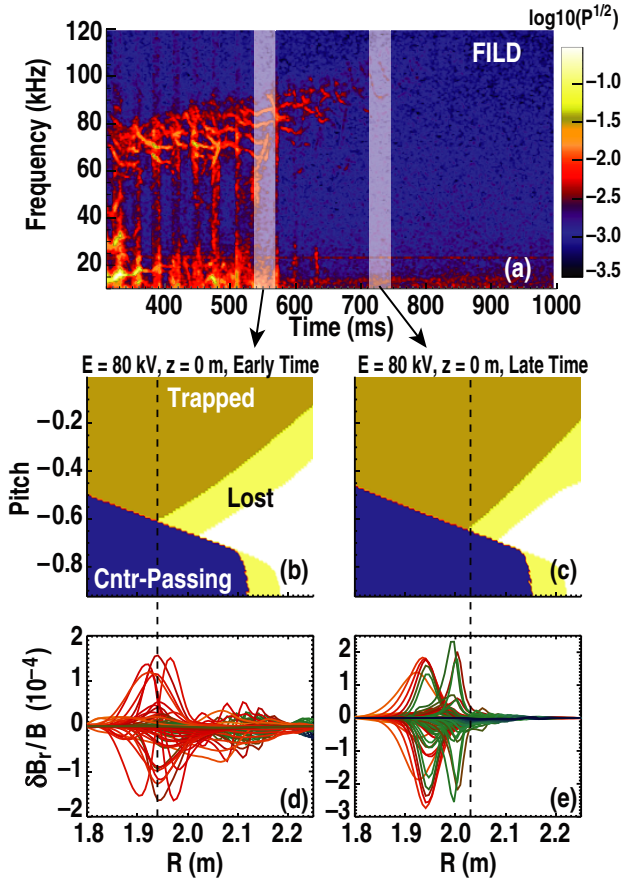

Figure 5. (*a*) FILD spectrogram showing coherent AE induced losses between 40 and 100 kHz during current ramp portion of discharge. Comparison of the loss boundaries and orbit topologies at 80 kV along the outboard midplane for the (*b*) 'early' time case and (*c*) 'late' time case. Yellow and white represent regions from which particles would be lost if launched with energy 80 kV at the corresponding radius and pitch along the outboard midplane. The corresponding eigenmodes along the outboard midplane are shown in (*d*) and (*e*), respectively. The dashed vertical line shows the innermost extent of the loss boundaries in each case.

in radius far more extensively at earlier times, making it much easier for them to transport particles to loss orbits.

3. Modelling of Alfvén eigenmodes and fast ion loss in ITER steady-state plasmas

Having seen that we are able to predict with some confidence the spectrum of unstable Alfvén eigenmodes as well as their ability to cause fast ion loss, the same techniques will now be applied to a simulated ITER DT steady-state plasma. This particular plasma is the ITPA IOS steady-state scenario 4 projection benchmark case [33]. The discharge is 8 MA with 5.3 T toroidal field and is heated by 33 MW of 1 MeV negative ion based neutral deuterium beams, 20 MW ICRF heating, 20 MW electron cyclotron heating. The profiles used as inputs to the modelling described here are shown in figures 6(*a*)–(*c*). The q-profile is reversed with $q_{\min} \approx 2.13$. A significant population of both 3.5 MeV alphas and deuterium beam ions is also present, with pressure profiles shown in figure 6(*c*). The actual fast ion distribution functions are calculated by TRANSP with the alphas having a typical isotropic slowing-down distribution whereas that of the beam ions is peaked in pitch near $\chi \approx 0.77$.

3.1. Eigenmode stability—ITER

Analogous to the process in section 2, NOVA was first used to calculate the eigenmodes of the ITER steady-state plasma for $n = 1$–15 then the stability of each mode was calculated using NOVA-K. The NOVA calculated Alfvénic continuum for all toroidal mode numbers considered is shown in figure 6(*d*), where the BAE, TAE and EAE gap are shown; however, calculations only considered modes in the TAE gap. Different from the DIII-D calculations, stability calculations for ITER included two separate ion species, beam ions and alphas. Future work will also include ICRF accelerated ions which may also lead to a non-negligible contribution to mode drive but was not included here due to lack of information about the actual RF created fast ion population.

Out of 566 distinct modes, three unstable modes in the TAE gap were found—$n = 5$ and $n = 6$ RSAEs and a $n = 6$ TAE. The displacement for the various poloidal harmonics of each mode on the outboard midplane as well as the real frequencies are shown in figure 7. Interestingly, the $n = 5$ RSAE is the fundamental radial mode whereas the $n = 6$ is the first radial harmonic. All of these modes are fairly localized near mid-radius with possibly the exception of the more global $n = 6$ TAE. These results are consistent with previous calculations performed for ITER baseline scenario plasmas [3] as well as reversed magnetic shear fusion development facility (FDF) plasmas [34] using NOVA-K. Modes localized near mid-radius are favoured due to the stronger fast ion pressure gradients in this region as well as increased ion Landau damping in the core and electron collisional damping at the edge.

What is notably different from previous ITER simulations is the shift to lower toroidal mode number for the modes predicted to be unstable. For baseline scenario cases ($q_{\min} \approx 1$), the strongest growing modes were in the range $n = 10$–11. This shift to lower n is actually expected for these high-$q_{\min}$ plasmas. Theoretically, fast ion drive increases with increasing toroidal mode number until the fast-ion gyroradius exceeds the width of the mode, with the most unstable toroidal mode number occurring near $k_\perp \rho_{\text{fast}} \approx 1$, where $k_\perp$ is the local poloidal AE wavenumber and ρ_{fast} is the fast ion gyroradius [36]. This implies, $n_{\max} \propto 1/q$, so, for higher $q_{\min}$, steady-state plasmas, $n_{\max}$ should be lower (approximately 1/2) as observed.

The contribution to the total drive from alphas and beam ions is shown in figure 8 as well as the contribution of the various damping mechanisms to the overall damping rates for the most unstable (or least stable modes). Peak growth rates are relatively large with the net drive exceeding the damping by approximately 50% for the most unstable $n = 6$ mode. Figures 8(*a*) and (*b*) show the surprising result that the largest drive for the modes is actually coming from the 1 MeV injected beam ions. Alphas, in fact, are providing only a small fraction of the overall drive. In retrospect, this may have been expected; the beam ion pressure gradient is actually larger near $q_{\min}$ (where the RSAEs are localized) and the 1 MeV beam ion

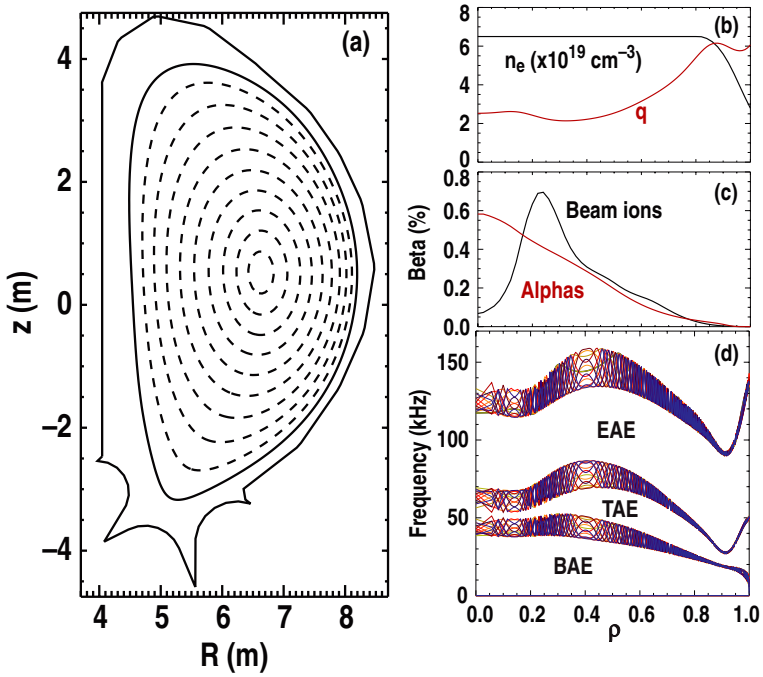

Figure 6. ITER steady-state scenario 4 plasma [33]. (*a*) Magnetic flux surface topology. (*b*) Electron density and safety factor profiles. (*c*) Alpha and beam ion pressure profile. (*d*) NOVA calculated Alfvénic continuum for all n.

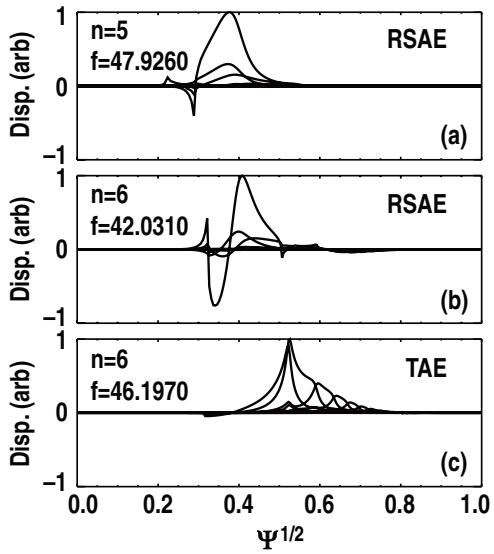

Figure 7. Modes in TAE gap predicted to be unstable for ITER steady-state scenario.

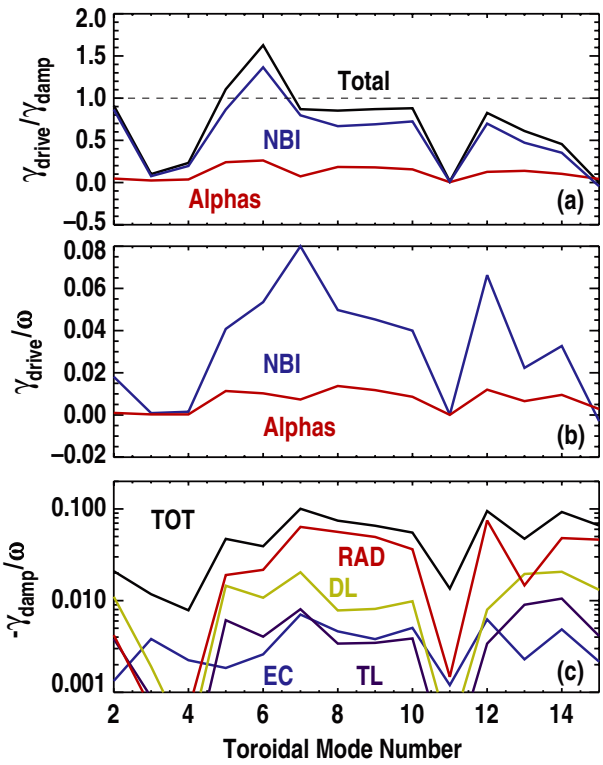

Figure 8. (*a*) Drive rate/damping rate for the most unstable or least stable mode as a function of toroidal mode number. Individual contribution from beam ions and alphas shown in blue and red, respectively. (*b*) Drive rate corresponding to panel (*a*). Total damping rate for modes in panel (*a*). Individual contribution from radiative (RAD), deuterium Landau (DL), tritium Landau (TL), and electron collision (EC) also shown.

speed is just above the Alfvén speed, $V_{NB}/V_A \approx 1.08$, whereas the alphas are born significantly above the Alfvén speed with $V_\alpha/V_A \approx 1.43$. The primary damping mechanisms are given in figure 8(*c*). For these modes, radiative damping is typically the largest, followed by thermal Landau damping. For many of the modes considered, electron collisional damping is also a large factor, primarily for modes extending to large minor radius. It is pointed out that the radiative damping model in NOVA-K was developed for TAE stability and is based on a circular plasma cross-section [35]. For RSAEs this model is more accurate near $q_{min} \approx (m - 1/2)/n$ and the top of their frequency sweep when the modes are more TAE-like.

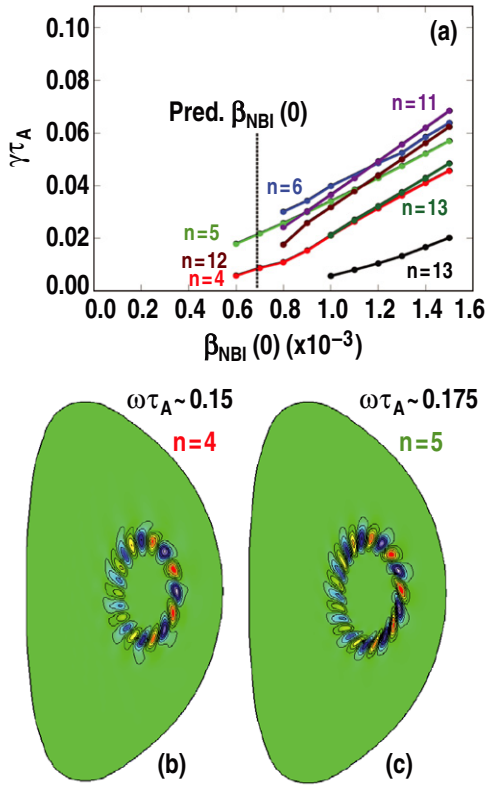

Figure 9. (*a*) TAEFL calculations for most unstable Alfvén eigenmode (for a given n) driven by beam ions as a function of central beam ion beta. Predicted central pressure delineated by vertical dashed line. (*b*) and (*c*) Structure of modes predicted to be unstable at predicted beam pressures. Note, the growth rates are expressed in terms of on-axis beam ion β, however, the beam ion pressure profile is peaked off-axis (as shown in figure 6(*c*)) with a value that is approximately a factor of 10 larger. The growth rates and real frequencies are expressed in terms of τ_A which is the characteristic Alfvén time on the axis ($\tau_A = R_0/v_{A0} \approx 6.27 \times 10^{-7}$ s).

Supplementing as well as providing a check on the NOVA-K stability calculations, simulations were carried out using the non-perturbative gyrofluid code TAEFL [18, 19]. TAEFL includes the fast ions as well as the primary damping mechanisms self-consistently but is able to treat only one fast ion species at a time as well as makes the assumption that each species is Maxwellian. Separate simulations for the alphas and beam ions were carried out and the most unstable mode found for a range of pressures. As with NOVA-K, no unstable modes were found when using alphas; however, when beam ions were considered, TAEFL finds similar results to NOVA-K. These results are shown in figure 9. Figure 9(*a*) shows the growth rate of the most unstable mode for a given toroidal mode number as a function of central beam ion pressure. At the predicted pressure values, $n = 4$ and $n = 5$ modes are found to be unstable with structures very similar to those found by NOVA. The 2D eigenmodes are shown in figures 9(*b*) and (*c*). At slightly higher pressure, an $n = 6$ mode is also found, similar to the $n = 6$ mode found by NOVA. Other noticeably higher n modes are found by TAEFL at higher pressures. These modes correspond to what appears to be EAEs localized near the inverted gradient region of the beam ion pressure profile and will be the subject of future investigations.

3.2. Fast ion loss—ITER

To answer the question of whether these unstable modes in ITER will be able to cause fast ion losses similar to those observed in present day devices, the same type of ORBIT simulations were carried out as for DIII-D discharge 142111 discussed in section 2.2. Beam ions and alphas sampled from the TRANSP distribution functions were followed in the presence of the modes shown in figure 7. In the DIII-D case, amplitudes were measured experimentally; for the ITER loss simulations, the mode amplitude is unknown so a range of amplitudes is considered. Simulations were carried out for amplitudes in the range $\delta B/B = 10^{-5}$–10^{-3}. For reference, in similar DIII-D discharges, typical observed mode amplitudes are $\delta B/B \approx 10^{-5}$–$10^{-4}$.

After following 10^6 particles including both alphas and beam ions for several milliseconds in the presence of the unstable mode spectrum, no lost particles were observed. To confirm these results, simulations were also carried out using the full-orbit following code SPIRAL [17] and the same result was obtained. Until mode amplitudes were increased to the $\delta B/B < 10^{-2}$ level, no losses were observed with ORBIT or SPIRAL.

The reason for this lack of fast ion loss can be understood by direct comparison with the DIII-D current ramp results shown in figure 5. To make connection with the DIII-D result, analogous orbit topology maps are shown for alphas and beam ions in figures 10(*a*) and (*b*), respectively. Figures 10(*c*) and (*d*) show the radial structure of the unstable eigenmodes on the outboard ITER midplane. As in the DIII-D case with little to no observed coherent loss in figures 5(*c*) and (*e*), the modes predicted to be unstable in ITER do not extend out to the innermost extent of the loss boundaries making fast ion loss directly due to these modes unlikely (although not plotted, the same conclusion holds for the inboard midplane).

4. Discussion and conclusions

In this paper, it was shown that NOVA-K linear stability calculations predict a similar spectrum of unstable modes to those observed in DIII-D current ramp experiments. ORBIT simulations using NOVA calculated eigenmodes reproduce many features of coherent DIII-D fast ion loss measurements. These simulations show the fast ion loss depends on proximity of modes to loss boundaries. When eigenmode stability calculations are carried out for an ITER reversed-magnetic shear steady-state plasma, unstable RSAEs and TAEs are found using both NOVA/NOVA-K and TAEFL. The modes predicted to be unstable are significantly lower toroidal mode number ($n = 4$–6) than the standard monotonic shear baseline case ($n \approx 10$) [3]. The unstable modes are relatively narrow radially and localized near mid-radius. It was also found that these unstable modes have the majority of their drive from deuterium beam ions (from 1 MeV injected heating beams) as opposed to alpha particles from fusion reactions. TAEFL and NOVA-K simulations also show EAE instability which will be discussed in future publications. For any reasonable range of mode amplitudes, both guiding-centre and full-orbit following codes show no coherent fast ion loss is expected due to these modes as observed in DIII-D, AUG, JET and other devices.

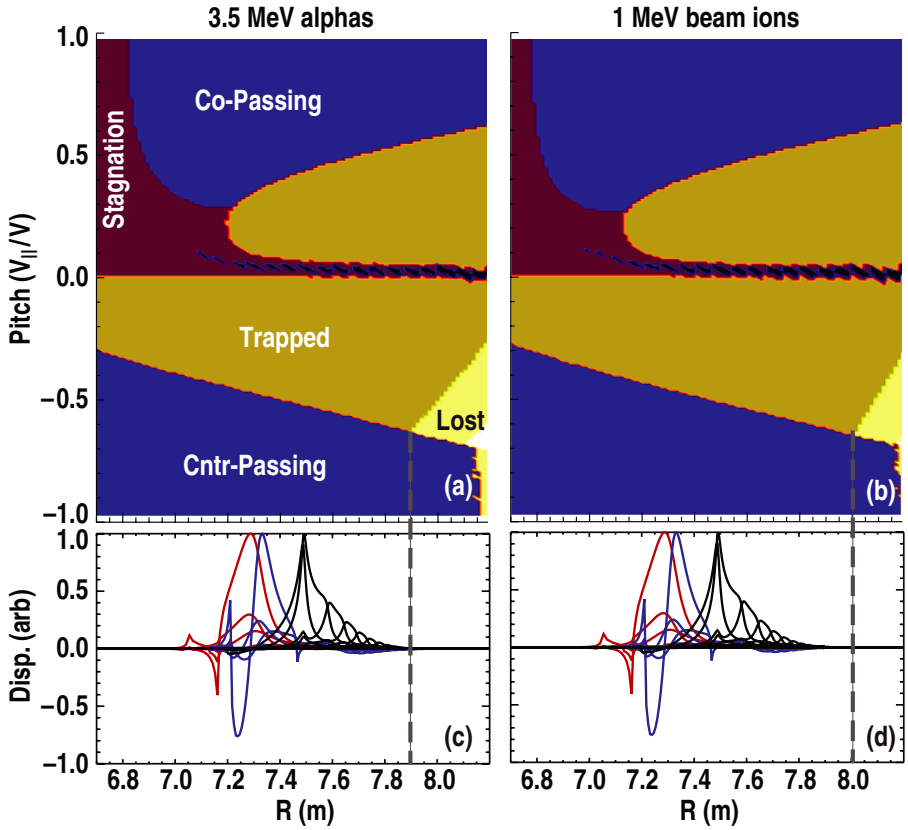

Figure 10. Comparison of the loss boundaries and orbit topologies along the outboard midplane for the (*a*) 3.5 MeV alpha and (*b*) 1 MeV beam ions. Yellow and white represent regions from which particles would be lost if launched with the corresponding radius and pitch along the outboard midplane. The corresponding radial structure of the NOVA-K predicted unsaddle eigenmodes are shown in (*c*) and (*d*). The dashed vertical line shows the innermost extent of the loss boundaries in each case.

This result can be explained by the smaller relative banana widths in ITER causing loss boundaries only at large radii and significantly removed from the modes themselves (as in the later time DIII-D case presented in figure 5). It is important to point out that these loss simulations apply to a specific aspect of fast ion losses—namely whether one expects losses due to these modes alone. Other modes or error fields (such as that from TBMs, ripple, or ELM mitigation coils) can significantly modify this result and increase the potential of these AEs to cause loss. Additionally, redistribution due to these modes will almost certainly occur and this causes changes in stability and the potential to drive other modes closer to loss boundaries, something which is not taken into account. Further, inclusion of scattering in the simulations (not discussed) causes a steady flux of incoherent loss and redistribution due to the modes can increase this incoherent flux of fast ions scattered across loss boundaries. These additional effects as well as the impact of RF tail ions on mode stability should be the subject of future work in the area.

Acknowledgments

This work was supported in part by the US Department of Energy under DE-FC02-04ER54698, DE-AC02-09CH11466, SC-G903402, DE-AC05-00OR22725 and DE-FG03-97ER54415.

References

[1] Wong K.L. 1999 *Plasma Phys. Control. Fusion* **41** R1
[2] Heidbrink W.W. *et al* 2008 *Phys. Plasmas* **15** 055501
[3] Gorelenkov N.N. *et al* 2003 *Nucl. Fusion* **43** 749
[4] Vlad G., Briguglio S., Fogaccia G., Zonca F. and Schneiderl M. 2006 *Nucl. Fusion* **46** 1
[5] Heidbrink W.W. *et al* 2007 *Phys. Rev. Lett.* **99** 245002
[6] Heidbrink W.W. *et al* 2008 *Nucl. Fusion* **48** 084001
[7] Garcia-Munoz M. *et al* 2010 *Phys. Rev. Lett.* **104** 185002
[8] Nabais F. *et al* 2010 *Nucl. Fusion* **50** 084021
[9] Fredrickson E.D. *et al* 2003 *Phys. Plasmas* **10** 2852
[10] Van Zeeland M.A. *et al* 2011 *Phys. Plasmas* **18** 056114
[11] Duong W.W., Heidbrink W.W., Petrie T.W., Lee R., Moyer R.A. and Watkins J.G. 1993 *Nucl. Fusion* **33** 749
[12] Nazikian R. *et al* 2008 *Phys. Plasmas* **15** 056107
[13] Pankin A. *et al* 2004 *Comput. Phys. Commun.* **159** 157
[14] Cheng C.Z. and Chance M.S. 1987 *J. Comput. Phys.* **71** 124
[15] Cheng C.Z. 1992 *Phys. Rep.* **211** 1
[16] White R.B. and Chance M.S. 1984 *Phys. Fluids* **27** 2455–67
[17] Kramer G.J. *et al Proc. 22nd Int. Conf. on Fusion Energy Conf. 2008 (Geneva, Switzerland, 2008)* CD-ROM file IT/P6-3 and http://www-naweb.iaea.org/napc/physics/FEC/FEC2008/html/index.htm
[18] Spong D.A., Carreras B.A. and Hedrick C.L. 1992 *Phys. Fluids* B **4** 3316
[19] Spong D.A., Carreras B.A. and Hedrick C.L. 1994 *Phys. Plasmas* **1** 1503
[20] Pace D.C. *et al* 2011 *Plasma Phys. Control. Fusion* **53** 062001
[21] Nazikian R. *et al* 2008 *Phys. Rev. Lett.* **101** 185001
[22] Fisher R.K., Pace D.C., Garcia-Munoz M., Heidbrink W.W., Muscatello C.M., Van Zeeland M.A. and Zhu Y.B. 2010 *Rev. Sci. Instrum.* **81** 10D307

[23] Pace D.C. *et al* 2010 *Rev. Sci. Instrum.* **81** 10D305
[24] Van Zeeland M.A. *et al* 2006 *Phys. Rev. Lett.* **97** 135001
[25] Van Zeeland M.A. *et al* 2007 *Phys. Plasmas* **14** 056102
[26] Van Zeeland M.A. *et al* 2009 *Nucl. Fusion* **49** 065003
[27] Tobias B. *et al* 2011 *Phys. Rev. Lett.* **106** 075003
[28] Nazikian R. *et al* 2006 *Phys. Rev. Lett.* **96** 105006
[29] Lao L.L., St John H.E., Stambaugh R.D., Kellman A.G. and Pfeiffer W. 1985 *Nucl. Fusion* **25** 1611
[30] Gorelenkov N.N., Cheng C.Z. and Fu G.Y. 1999 *Phys. Plasmas* **6** 2802
[31] Austin M.E. and Lohr J. 2003 *Rev. Sci. Instrum.* **74** 1457
[32] Tobias B. *et al* 2010 *Rev. Sci. Instrum.* **81** 10D928
[33] ITER SS Scenario Benchmark Simulation Guideline V1.0 (december 4, 2009) NBI benchmark, EDA2001 design, Oikawa IAEA 2008
[34] Chan V. *et al* 2009 *Fusion Sci. Technol.* **57** 66–93
[35] Fu G.Y. *et al* 1996 *Phys. Plasmas* **3** 4036
[36] Heidbrink W.W. 2002 *Phys. Plasmas* **9** 2113